10216–10224 *Nucleic Acids Research, 2018, Vol. 46, No. 19* *Published online 17 September 2018*
doi: 10.1093/nar/gky826

A single molecule analysis of H-NS uncouples DNA binding affinity from DNA specificity

Ranjit Gulvady[1], Yunfeng Gao[1], Linda J Kenney[1,2,3,4] and Jie Yan[1,5,6,*]

[1]Mechanobiology Institute, National University of Singapore, Singapore 117411, Singapore, [2]Jesse Brown Veterans Administration Medical Center, Chicago, IL 6061, USA, [3]Department of Microbiology and Immunology, University of Illinois-Chicago, Chicago, IL 60612, USA, [4]Department of Biochemistry, National University of Singapore, Singapore 117596, Singapore, [5]Department of Physics, National University of Singapore, Singapore 117542, Singapore and [6]Centre for Bioimaging Sciences, National University of Singapore, Singapore 117546, Singapore

Received July 21, 2018; Revised September 03, 2018; Editorial Decision September 05, 2018; Accepted September 06, 2018

ABSTRACT

Heat-stable nucleoid structuring protein (H-NS) plays a crucial role in gene silencing within prokaryotic cells and is important in pathogenesis. It was reported that H-NS silences nearly 5% of the genome, yet the molecular mechanism of silencing is not well understood. Here, we employed a highly-sensitive single-molecule counting approach, and measured the dissociation constant (K_D) of H-NS binding to single DNA binding sites. Charged residues in the linker domain of H-NS provided the most significant contribution to DNA binding affinity. Although H-NS was reported to prefer A/T-rich DNA (a feature of pathogenicity islands) over G/C-rich DNA, the dissociation constants obtained from such sites were nearly identical. Using a hairpin unzipping assay, we were able to uncouple non-specific DNA binding steps from nucleation site binding and subsequent polymerization. We propose a model in which H-NS initially engages with non-specific DNA via reasonably high affinity (~60 nM K_D) electrostatic interactions with basic residues in the linker domain. This initial contact enables H-NS to search along the DNA for specific nucleation sites that drive subsequent polymerization and gene silencing.

INTRODUCTION

Bacterial DNA can be anywhere between 300 kb (1,2) to over 14 Mb (3), which when fully stretched, has a length that is in the order of millimetres. Given that the size of bacteria is itself in the range of a few microns, bacteria require a mechanism to condense the chromosomal DNA within the cell in a way that allows for various transcations on DNA, such as transcription and replication, to take place. The physical organization of chromosomal DNA in cells is achieved by a class of DNA binding proteins referred to as nucleoid-associated proteins (NAPs) (4–6). Apart from assisting in the physical organization of DNA, NAPs also play an important role in global gene regulation (7,8).

One such NAP that is essential for gene silencing is the heat-stable nucleoid structuring protein (H-NS) (9–11). H-NS is present at ~20 000 copies per genome during the exponential phase (12–14), and has a relatively small size of ~15 kDa. Previous *in vitro* studies have demonstrated that H-NS can exist in various oligomeric states depending on the concentration of H-NS, with an H-NS dimer as the minimal functional form (15). Formation of H-NS dimers or higher order oligomers occurs via two dimerization interfaces present in the N-terminus of H-NS (16). Importantly, previous single-molecule studies have revealed that H-NS can form a continuous filament on DNA driven by oligomerization (17–20). This filament formation is crucial for the gene silencing function of the H-NS family of proteins (21–25).

Previous results demonstrated that H-NS family proteins have a preference to bind to certain A/T-rich sequence motifs that are present in promoter regions of genes that are silenced by H-NS (26–30). These sequence motifs have been proposed to act as nucleation sites for H-NS (31), allowing formation of local H-NS filaments that results in gene silencing (25). DNase I footprinting has identified a high affinity site in the *proU* promoter of *E. coli*. This site was shown to be necessary for H-NS to initially bind and then spread across the DNA to establish the nucleoprotein filament structure. (32). These results raised questions as to how the H-NS filament extends from such nucleation sites and stabilizes the filament.

In order to understand gene silencing by H-NS, it is important to understand the role of the individual domains of H-NS in DNA binding. H-NS has three major domains: an N-terminal oligomerization domain contains two dimerization sites (33), a C-terminal DNA binding domain (33,34), and a flexible, unstructured linker joins these two domains

*To whom correspondence should be addressed. Tel: +65 6516 2620; Email: phyyj@nus.edu.sg

(35). Previously the linker domain was mainly thought to play a passive role in providing flexibility between the N- and C-termini. However, a recent study determined that substitution of the five basic residues in the highly conserved linker domain with charge-neutral residues completely abolished gene silencing, as well as filament formation on DNA (36).

These results indicated that the linker domain plays a crucial role in H-NS gene silencing, not only through the flexibility it provides, but also through a yet to be determined mechanism.

To provide insight into the molecular mechanisms underlying H-NS filament formation around the nucleation sites and the role of the linker domain, we developed a highly sensitive label-free single-molecule approach to quantify H-NS binding to short DNA sequences, similar to (37,38). Our study provides several important findings: (i) basic residues in the linker domain are the largest contributors to DNA binding affinity, (ii) nucleation sites increase the binding affinity by 3-6-fold compared to non-specific sequences of the same length, (iii) the nucleation site serves as a crucial anchoring point to form a local H-NS filament that is highly dynamic in nature and (iv) although H-NS is reported to prefer A/T-rich DNA compared to G/C-rich DNA, its binding affinity is nearly identical. Taken together, our study provides a more comprehensive understanding of the molecular mechanisms that underlie gene silencing by H-NS.

MATERIALS AND METHODS

Protein and DNA preparation

Wild type (wt) H-NS and three mutants (Q15, KR2 and K2R2) were prepared as described previously (36). For the Q15 mutant, the linker of the wt-H-NS was replaced with a 15 amino acid sequence of the charge-neutral polyglutamine. The two additional linker mutants, KR2 and K2R2, were prepared by adding back a different number of charged residues to the Q15 linker. All oligonucleotides were purchased from Integrated DNA Technologies. Designing the DNA construct involved three basic steps: PCR of the double-stranded DNA (dsDNA) handle and its restriction enzyme cutting, annealing of the hairpin oligonugleotides wih the linker, and ligation of the handle with the annealed hairpin-linker product. The 5′-thiol labeled 600 basepair (bp) dsDNA handle was prepared by PCR using Q5 Hot Start High-Fidelity DNA Polymerase on a lambda phage template (New England Biolabs). PCR products were purified using the Thermo Scientific kit and digested with BsaI-HF restriction enzyme (NEB) at 37°C for 1 h. The hairpin oligonucleotides and linker were annealed by mixing equal amounts of the oligonucleotides and incubating in a water bath at 95°C for a few seconds, after which the water bath was switched off, and the water was allowed to come down to room temperature over 7-8 hours. The annealed linker-hairpin complex and the digested dsDNA handle were then ligated using the T4 DNA ligase (NEB). Sequences of all the DNA oligonucleotides used are listed in Supplementary Data under 'DNA oligonucleotides'.

Single-molecule magnetic tweezers

A flow channel (volume ∼10–20 μl) was constructed on a (3-aminopropyl)triethoxy silane (APTES) (Sigma-Aldrich) functionalized coverslip (32 × 22 mm). The channel was incubated with the sulfo-SMCC crosslinker (dissolved in 1× phosphate buffered saline (PBS) buffer, pH 7.4) for 30 min. After washing out the unbound sulfo-SMCC, the thiol-labeled DNA construct was introduced into the channel, and incubated for another 30 min. The thiol-end of the DNA construct was covalently attached to the amine group of APTES via this sulfo-SMCC crosslinker (Thermo Scientific). The channel was then blocked with bovine serum albumin (BSA) solution (10 mg/ml BSA, 1 mM 2-mercaptoethanol, 1× PBS saline pH 7.4 buffer) for at least 2 h before the experiment. For the experiment, 2.8 μm-diameter streptavidin coated paramagnetic beads (Dynal M-280, Life technologies) were incubated in the channel for ∼10 min to bind the biotinylated end of the DNA construct. For single-molecule stretching experiments, the working buffer (50 mM KCl, 10 mM Tris, pH 7.4) was flushed into the channel. All experiments were performed using these buffer conditions at 25°C.

Binding and cooperativity measurements

To quantify H-NS binding to DNA, the Hill equation was used:

$$\theta = \frac{1}{1 + (K_D/c)^n} \quad (1)$$

Here, θ = the fraction of H-NS bound to DNA, c = H-NS concentration, K_D = dissociation constant, n = Hill coefficient.

RESULTS

Delayed hairpin unzipping probes site-specific H-NS binding

We used magnetic tweezers to detect site-specific binding of H-NS based on delayed hairpin unzipping as depicted in Figure 1A. A DNA hairpin held by Watson-Crick base-pairing interactions can be destabilized by force when it exceeds a certain threshold, F_c, hereafter referred to as the critical force. The value of F_c is dependent on the DNA sequence, solution conditions and the terminal loop (39). Within a narrow force range around F_c, $\delta \sim k_B T/\Delta x$, both the unfolded and folded states have significant probabilities and therefore frequent two-state fluctuation is observed (Supplementary Figure S1). Here, k_B is the Boltzmann constant, T the temperature, and Δx is the stepsize of the hairpin unfolding at the critical force. The DNA predominantly exists in the unfolded state at forces above $F_c + \delta$, and in the folded state at forces below $F_c - \delta$. In an experiment where the force is increased from a small force ($\ll F_c$) to a force sufficiently above $F_c + \delta$, the hairpin will undergo a one-way unfolding transition (Figure 1A, right).

To ensure this one-way unfolding transition, in our experiments, a probing force, $F_p > F_c + \delta$ was employed such that the lifetime of the folded state was less than one second (Figure 1A, top left). If H-NS binding to the hairpin results in a significant delay in hairpin unfolding at F_p (Figure 1A,

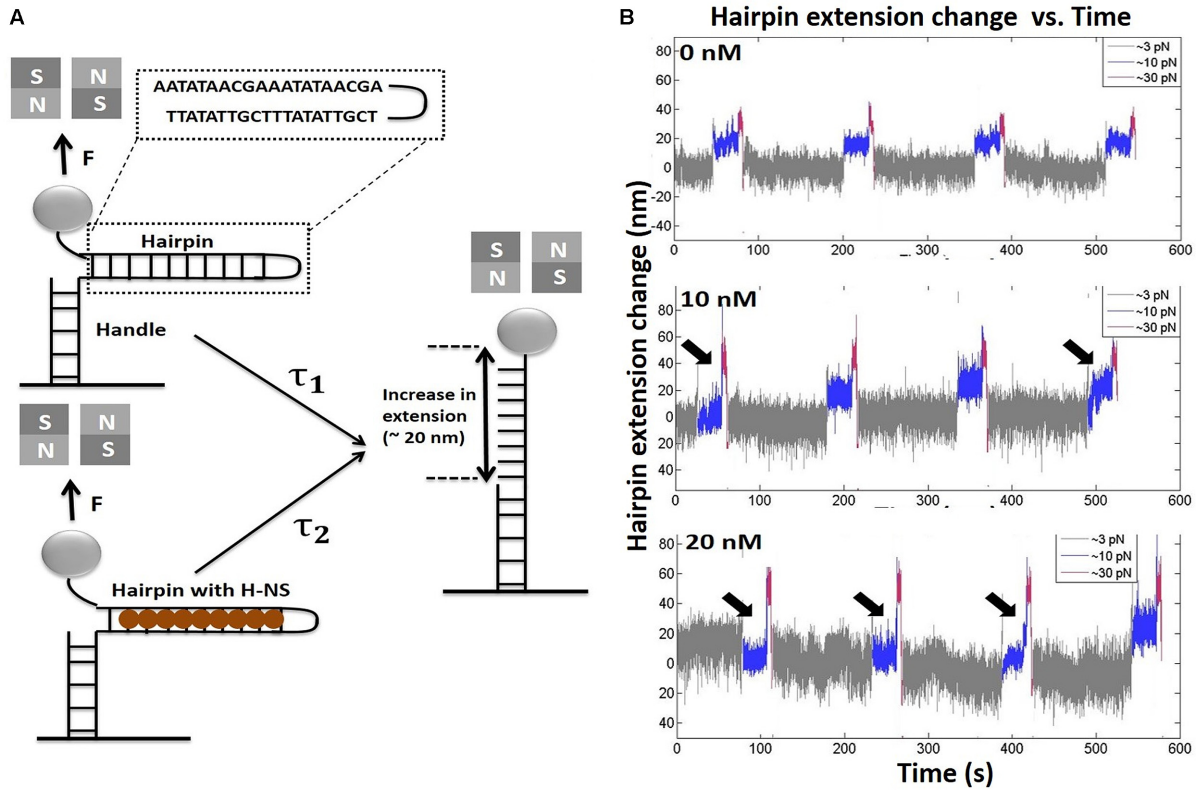

Figure 1. Quantification of H-NS-DNA binding affinity. (**A**) Schematic of the principle of the measurement. A force is applied on the hairpin using a pair of permanent magnets shown in grey (N: north pole, S: south pole). At a force slightly greater than the critical force, F_c, the naked DNA hairpin has a short lifetime of τ_1, while the hairpin bound with H-NS has a much longer lifetime of τ_2. This delayed unzipping indicates H-NS binding. (**B**) Representative time traces of the extension change of the *proU* 2xNS hairpin for three H-NS concentrations: 0 nM (top), 5 nM (middle) and 10 nM (bottom). The measurements were recorded at three forces: the binding force (~3 pN, grey, 2 min), at which the H-NS-hairpin complex reaches equilibrium, the probing force (~10 pN, blue, 30 s), slightly greater than F_c and the displacing force (~30 pN, magenta, 5 s), to rapidly displace bound H-NS. The black arrows indicate the cycles at which H-NS-DNA binding was observed.

bottom left), then the readout of the lifetime of the folded state at this force provides information as to whether H-NS was bound to the DNA or not before the hairpin unfolds. In order to apply this approach to measure the probability of H-NS binding to a DNA hairpin, we implemented repeated cycles of three forces: a binding force $F_b \ll F_c$ to allow the hairpin to interact with H-NS and undergo equilibrium binding, a probing force F_p as described earlier, to determine whether the hairpin was bound by H-NS, and a displacing force $F_d \gg F_c$ to instantly remove any bound H-NS and unfold the hairpin.

We first investigated H-NS binding to a 20 bp hairpin that contains two repeats of the *proU* nucleation site (*proU* 2xNS), and has a critical force of $F_c \sim 7$ pN (Supplementary Figure S1B). The binding, probing and displacing forces were selected to be $F_b \sim 3$ pN, $F_p \sim 10$ pN and $F_d \sim 30$ pN. The DNA was held at F_b for 2 min to ensure equilibrium binding, before jumping to F_p. At F_p, the DNA was held for 30 seconds to measure the lifetime of the hairpin. After this, the force was then further increased to F_d for 5 s to ensure dissociation of any H-NS bound to the DNA. By performing these series of steps in a cyclic manner, the probability of H-NS binding to the hairpin was then calculated as the fraction of the force cycles where H-NS binding was detected based on delayed hairpin unfolding. For any given DNA tether, at a given H-NS concentration, an experiment consisted of 30 such cycles.

Figure 1B (top) shows a representative time trace of the extension change of the hairpin before introducing H-NS, during four consecutive force cycles extracted from 30 cycles. The extension of the hairpin in the folded state is set as the reference (Supplementary Figure S2). The data in Figure 1B shows three distinct extensions during cycles of the three forces. After introducing 10 nM H-NS, delayed unfolding of the hairpin was observed in some of the cycles (e.g. the first and last cycle in Figure 1 B, middle, indicated by the black arrows). Such delays in unfolding became more frequent when the H-NS concentration was increased to 20 nM (e.g. the first three cycles in Figure 1B, bottom, indicated by the black arrows). Thus, by performing the experiments at different H-NS concentrations, one can measure the concentration-dependent probability of binding from which the DNA binding affinity can be quantified.

Quantification of sequence-dependent H-NS binding

In this section we applied the above described method to investigate sequence-dependent H-NS binding. The minimal functional form of H-NS is a dimer (15). A more recent study suggested that each H-NS dimer occupied nearly two helical turns of DNA (16). Therefore, the hairpins used in

our study were selected to have a 20 bp stem, which provides a single binding site for an H-NS dimer.

Four sequences were used for the current study. One was *proU* 2xNS, containing the two repeats of the 10 bp high affinity H-NS nucleation site from the *proU* promoter in *Escherichia coli* (32). The second sequence contained a 10 bp repeat of the H-NS nucleation site in the *csgD* promoter in *E. coli* (*csgD* 2xNS) (40). Both the *proU* and the *csgD* sites have 80% A/T content. The other two nonspecific sequences, one with 80% A/T content (AT control) and the other with 50% A/T content (GC control), were selected to examine the roles of A/T-rich DNA in the binding affinity of H-NS.

In Figure 2A, the probability of H-NS binding to *proU* 2xNS is shown at different H-NS concentrations. The final probability values obtained represents the average value across five independent DNA tethers, along with the corresponding standard error. Fitting the average binding probability vs. H-NS concentration with the Hill equation determined the dissociation constant, K_D, to be 10.2 ± 0.5 nM with a Hill coefficient, n, of 2.18 ± 0.24. The K_D and the Hill coefficient for the other sequences were similarly determined as follows: $K_D = 22.2 \pm 0.5$ nM and $n = 3.31 \pm 0.24$ for *csgD* 2xNS (Figure 2B), $K_D = 56.9 \pm 3.0$ nM and $n = 2.94 \pm 0.45$ for the AT control (Figure 2C), and $K_D = 59.8 \pm 5.1$ nM and $n = 2.10 \pm 0.41$ for the GC control (Figure 2D). Interestingly, although it is widely recognized that H-NS selectively prefers A/T-rich DNA, the discrimination between G/C and A/T DNA only resulted in a 3 nM difference in binding affinity (see Discussion).

These results clearly show that the binding affinity of H-NS to the *proU* and *csgD* nucleation sites was significantly higher (3-6-fold) than the two non-specific sequences (Figure 2). This result was consistent with a role of these nucleation sites in recruiting H-NS to the *proU* and *csgD* promoters for gene silencing. For all of the sites, the Hill coefficient was in the range of 2–3. A Hill coefficient with a value larger than one indicates positive binding cooperativity. In our case, this cooperativity comes from the binding of a single H-NS dimer. Comparison between the *proU*, *csgD* and the A/T-rich nonspecific hairpin having the same A/T content revealed that A/T content alone is not a determining factor of H-NS DNA binding affinity. This was further supported by the similar affinity between the two nonspecific sequences with very different A/T content.

The linker domain is crucial for H-NS DNA binding affinity

Previous studies have shown that H-NS binding to DNA was strongly dependent on the salt concentration (19), suggesting that an electrostatic interaction between H-NS and DNA was crucial for its binding affinity. A recent study revealed that the linker domain (15 amino acids) played a critical role in H-NS mediated gene silencing *in vivo*, which interestingly depended on several lysine and arginine residues (36). This raised an important question concerning the functional roles of these charged residues in the linker domain. We hypothesised that these residues might have a significant impact on the overall binding affinity of H-NS to DNA, and we tested this hypothesis using the above described single-molecule approach.

To test the hypothesis, we prepared various H-NS mutant proteins with different linkers, including the wt linker, a linker substituted with a 15 amino acids charge-neutral poly-glutamine (Q15 mutant), and two additional linker mutants, KR2 and K2R2, with a different number of charged residues added back to the Q15 linker (Figure 3A). Our previous study showed that the Q15 mutant completely lost its gene silencing function while the KR2 and K2R2 mutants partially recovered gene silencing (36). The binding affinity of H-NS with each of these different linkers was measured using the *csgD* 2xNS hairpin.

Figure 3B shows that the K_D measured for the Q15 mutant was 1522.2 ± 54.5 nM, indicating a 70-fold decrease in the binding affinity compared to the wt H-NS. In Figure 3C and D, the binding curves for the KR2 and K2R2 mutants are shown. From these data, the K_D values of these mutants were determined to be 433.4 ± 8.1 and 108.2 ± 3.6 nM, respectively. These results demonstrate that the charged residues in the linker domain indeed play a crucial role in determining the binding affinity of H-NS, and substitution of the charged residues reduced affinity by 70-fold (Figure 3 B) and eliminated gene silencing (36). For all of the cases, the Hill coefficients were >2, indicating that the cooperativity of H-NS binding was not dependent on the charged residues of the linker (See Discussion).

H-NS nucleation and polymerization is evident in the hairpin unzipping assay

We next investigated the local spreading (polymerization) of the H-NS filament from a nucleation site. Performing our experiments at the single-molecule level ensured bp resolution to precisely monitor the extent of H-NS polymerization along the DNA, a feature that was missing in previous H-NS spreading studies (32).

To observe spreading of the H-NS filament, we used a DNA construct containing a 70 bp hairpin. This hairpin contains the 10 bp *proU* nucleation site in the center, with 30 bp of nonspecific DNA sequence on either side of the nucleation site (Figure 4A). We refer to this hairpin as *proU* 1xNS. A representative time trace of the extension change of the hairpin in the presence of 20 nM H-NS exhibited strong binding signals (Figure 4B). Zooming into one such binding signal revealed partial unfolding and refolding of the hairpin (Figure 4B, inset). This indicated that the DNA was partially covered by H-NS, and unzipping of DNA was prevented by the first stably bound H-NS complex away from the fork containing the fully hybridized hairpin (e.g. in the blue region to the left of the orange nucleation site in Figure 4A). Since H-NS binding to DNA is cooperative (Figure 2), large tracts of continuous filament are formed (17–19). Therefore, we reasoned that unzipping is prevented at the end of a stable H-NS filament.

To quantify the precise position of the end of the filament, distributions of the DNA extension after jumping from ∼3 to ∼13 pN in the absence and presence of H-NS were analyzed. In the absence of H-NS, the hairpin opened instantaneously. This resulted in a narrow distribution of the extension, with a single peak at an extension of ∼69 nm (Figure 5 A), consistent with the expected value from a fully unzipped DNA (Supplementary Data — 'ssDNA extension

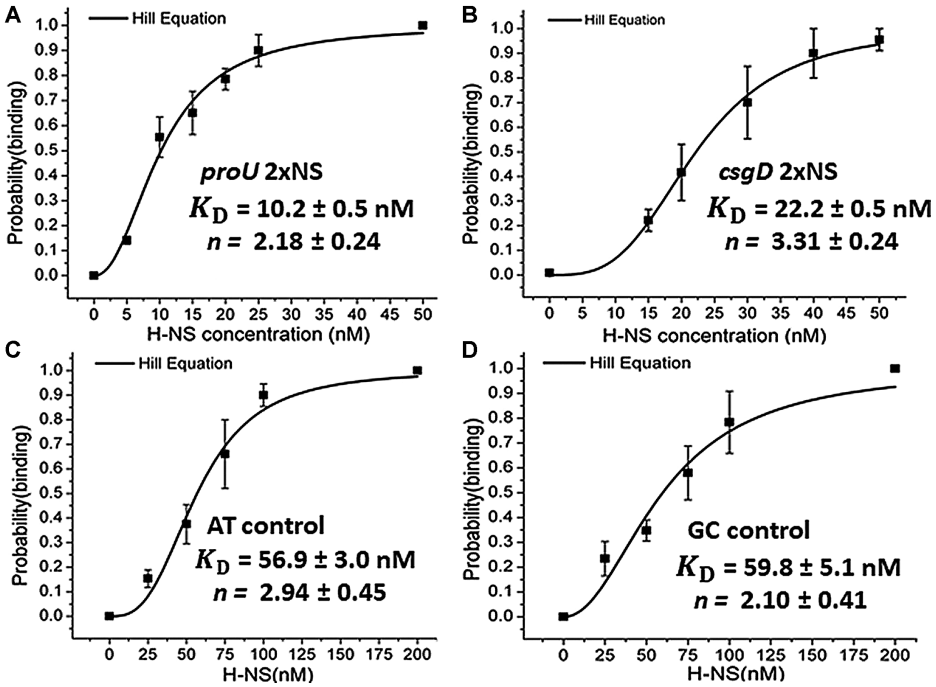

Figure 2. Sequence-dependent H-NS binding to DNA. The equilibrium binding probability as a function of H-NS concentration was plotted for (**A**) *proU* 2x NS, (**B**) *csgD* 2x NS, (**C**) AT control and (**D**) GC control. The solid curves are the fitted curves to the Hill equation.

change'). In the presence of 5 nM H-NS, unzipping was delayed, indicating H-NS binding. Unzipping was apparent in 29% of 150 cycles from five, independent tethers. The extension distribution at the high force (∼13 pN) contained three peaks at ∼0, ∼27 and ∼70 nm, respectively (Figure 5B, inset). The peak at ∼0 nm resulted from an H-NS polymer ending near the fork of the fully hybridized hairpin. The peak at ∼27 nm resulted from H-NS spreading up to 29 bp from the fork (Supplementary Data — 'ssDNA extension change'), i.e. close to the *proU* nucleation site, located 30 bp from the fork. Together, these results revealed a bistable distribution of the filament end from the fork.

When the H-NS concentration was increased to 20 nM, increased H-NS binding was observed (81% of the cycles). Despite the increased probability of binding, the extension distribution at ∼13 pN (based on data obtained in all the cycles) still exhibited three peaks at similar positions (Figure 5 C). The probability of the filament ending near the fork was increased 6-fold, and around the nucleation site by 2-fold, compared to 5 nM H-NS. Overall, these results indicated that increasing the H-NS concentration did not affect the bistable filament localization, but it increased the overall frequency of nucleation and polymerization of H-NS.

To probe the role of the basic residues in the linker domain on the observed three-peak profile, we repeated the experiment using the Q15 mutant (Figure 5D–F). As shown in Figure 5E, binding was barely detected at H-NS concentrations up to 2 μM. In spite of the significantly higher concentrations of H-NS required for binding, the three-peak profile remained visible at the same positions (Figure 5F) as observed with wt H-NS (Figure 5B and C). This result indicated that the linker substitutions altered the binding affinity without affecting either sequence recognition (nucleation site binding), or the nature of spreading of H-NS from the nucleation site (polymerization).

We also investigated the role of the nucleation site on the observed three-peak profile. We performed identical experiments on a control 70-bp DNA hairpin of the same A/T:G/C ratio lacking the *proU* nucleation site (Figure 5G–I). We discovered that at an H-NS concentration of 20 nM , binding signals were barely detected (Figure 5H). This was in sharp contrast to the results obtained with *proU* 1xNS at the same concentration, where a clear binding signal was observed (Figure 5C). Increasing the H-NS concentration to 80 nM enabled binding to the control hairpin (Figure 5I). However, only a two-peak distribution was observed, in contrast to the three-peak profiles observed in Figure 5C and F. The middle peak, corresponding to the nucleation site, was missing. This result suggested that the *proU* nucleation site indeed serves a role to nucleate the binding and subsequent polymerization of H-NS.

DISCUSSION

In this study, we developed a highly-sensitive single-molecule technique that enabled the precise quantification of protein binding to short DNA sequences. Our results provide some key insights into the molecular mechanism that governs the formation of H-NS filaments on DNA and leads to gene silencing. Binding studies of H-NS to the nucleation site of the *proU* and *csgD* promoters of *E. coli* revealed an increase in the binding affinity by ∼ 3-6-fold compared to similarly designed non-specific sequences. We observed that basic residues in the linker domain surprisingly made the greatest contribution to the DNA binding affinity of H-NS (36,41). We determined that a nucleation site

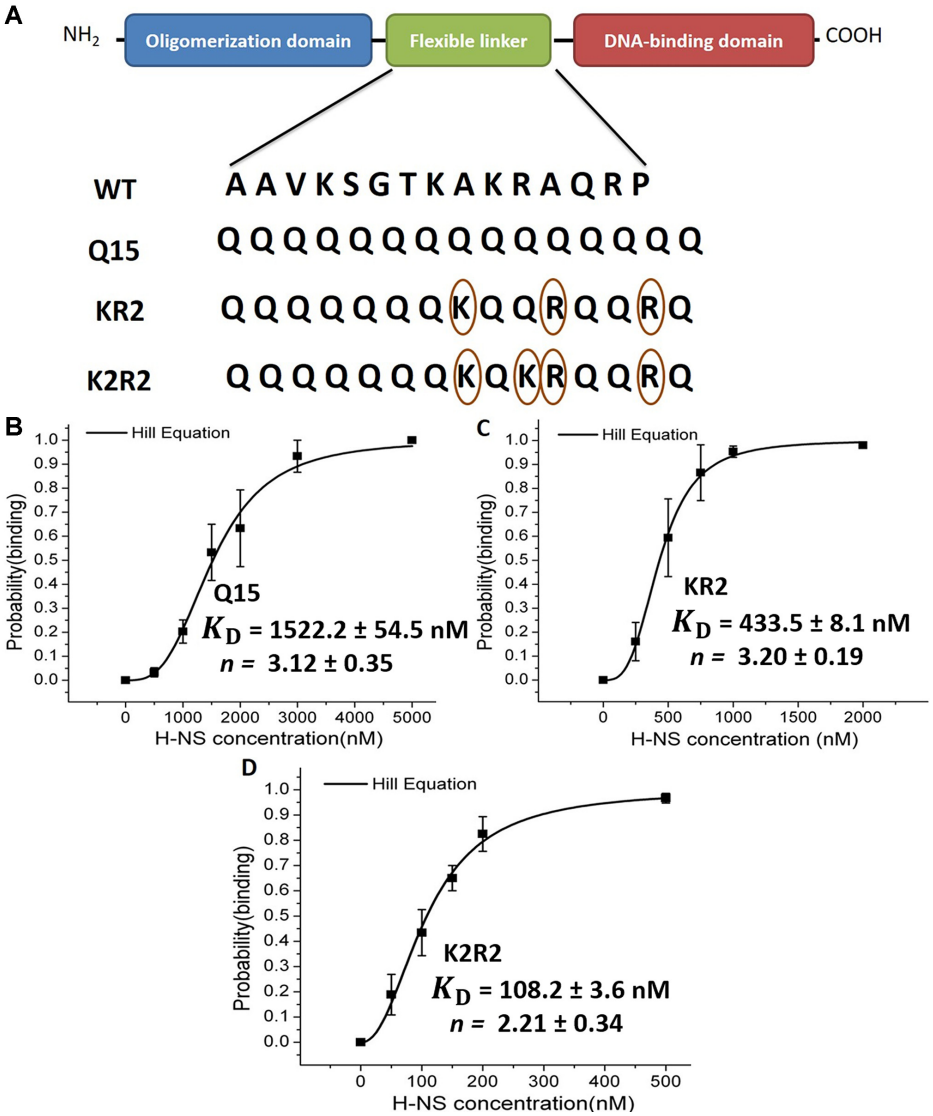

Figure 3. Effects of charged residues in the linker domain on H-NS binding affinity. (**A**) Schematic of the domain map of H-NS. The residues in the linker domain for wt and the three mutants. The brown circles indicate the charged residues. (**B**–**D**) Quantification of binding affinity of (B) Q15 mutant (C) KR2 mutant (D) K2R2 mutant.

serves as an anchoring point for the formation of locally spread, highly dynamic H-NS filaments. This nucleation behavior was also evident in the Q15 linker mutant (Figure 5F), which bound to DNA with a 70-fold lower affinity compared to wt HNS (Figure 3 B). Thus, DNA binding affinity was uncoupled from nucleation.

Interestingly, our experiments with the 80% A/T and 50% A/T-rich control sequences demonstrated that the change in A/T-content did not have a significant effect on binding affinity. This was surprising, because so many studies state a preference of H-NS for A/T-rich DNA (26–29). However, the apparent dissociation constants obtained for DNA hairpins containing *proU* or *csgD* nucleation sites were 3-6-fold lower than the control sites, highlighting the importance of the nucleation site in directing H-NS binding to relevant promoter regions for gene silencing.

We discovered that H-NS binding to DNA was highly sensitive to the presence of basic residues in the linker domain (36,41). Our study quantified the linker contribution to the DNA binding affinity and showed that DNA binding by the linker region is critically dependent on the charged residues in the linker. Complete replacement of the linker reduced the binding affinity by ∼ 70-fold, but the original binding affinity was mostly recovered upon reintroducing the basic linker residues (Figure 3). The importance of the linker domain in DNA binding was originally discovered by Shindo *et al.* (41). Their results revealed that when the entire N-terminal domain (1–80) is deleted, the binding affinity of the mutant is reduced by 25 folds compared to full-length H-NS (41). This is less than the ∼70-fold affinity decrease observed for the Q15 linker mutant in our experiment. Thus, we can conclude that the linker region (80–94) has a greater contribution to the DNA binding affin-

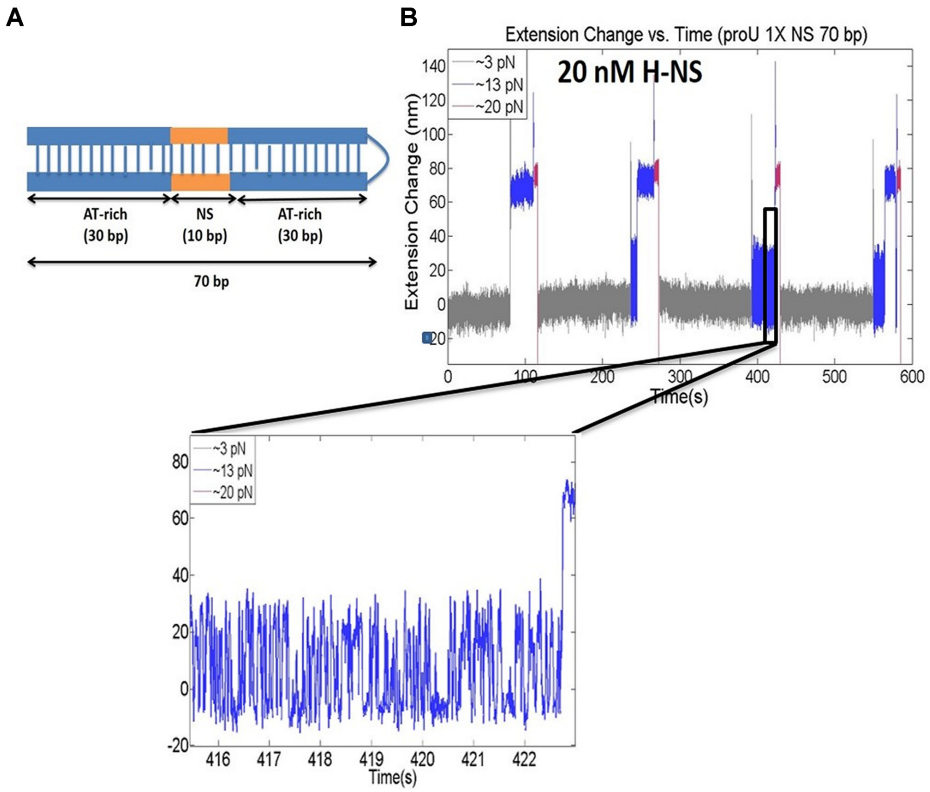

Figure 4. Partial H-NS binding to the DNA. (**A**) Schematic of the 70 bp hairpin (*proU* 1xNS, 70 bp) used to observe H-NS spreading. The *proU* nucleation site (orange) is in the center. (**B**) Representative time trace of the extension change of the hairpin at 20 nM H-NS. At the probing force of ∼13 pN, partial hairpin unzipping indicates partial H-NS binding (inset).

ity than the N-terminal domain (1–80). Furthermore, although the data wasn't provided, Shindo *et al.* mentioned that the DNA binding affinity of the C-terminal region (91–147) is about 1/2000 of that of the wild type H-NS. In that experiment, the entire N-terminus and the first 11 residues in the linker region were deleted. This result suggests that the region encompassing the N-terminal domain (1–80) and 11 residues in the linker region (80–90) is most likely the primary contributor to the binding affinity of H-NS compared to the C-terminal region (91–147). Together with the consideration that the linker region is a greater contributor to binding affinity than the N-terminal domain, the following order of the affinity contribution can be established: the linker region (80–94 aa) > N-terminal domain (1–80) > C-terminal domain (91–147). These results directly demonstrate that the H-NS linker domain is the main determinant to the DNA binding affinity of H-NS. Previously, the linker domain was mainly considered to play a passive role in providing flexibility between the N- and C-termini. Our result therefore reveals a new function of the linker domain (36).

On the other hand, the linker domain does not convey sequence specificity due to the pure electrostatic nature of the linker-DNA interaction. Thus, these two features can be uncoupled from one another, as we demonstrated (Figures 3 and 5). Therefore, there must be an additional DNA binding mechanism to explain why H-NS preferentially silences genes with promoters containing certain consensus nucleation sites (31). Previous studies have shown that the C-terminus of H-NS is a DNA binding domain (33,34). This domain contains a conserved Q/RGR motif that selectively interacts with the DNA minor groove, which was suggested to regulate the sequence-dependence of DNA binding by H-NS (42). Together with these previous results, we propose that the linker domain brings H-NS to DNA electrostatically and independent of DNA sequence. This then allows H-NS to search for the nucleation sites on the DNA that are recognized by the C-terminal domain (36).

We also examined the local spreading (polymerization) of the H-NS filament from the nucleation site by probing the boundary between an H-NS nucleoprotein filament and the naked DNA from the entry of a DNA hairpin (Figure 5). Overall, our results provide evidence that a nucleation site indeed localizes H-NS binding and promotes local spreading of the filament around the site. Consistent with this view, on a control DNA hairpin that lacked a nucleation site, the H-NS filament still formed, but required a 4-fold higher H-NS concentration compared to the DNA hairpin that contained a nucleation site. In addition, the spreading of the filament originated randomly and not from any specific location.

In summary, we employed a highly-sensitive hairpin unzipping assay to determine single-site binding affinities of H-NS. Using this approach, we could directly compare H-NS mutants that were deficient in binding. Furthermore, we could uncouple high affinity binding and sequence-specific binding. Taken together, our study provides an enhanced

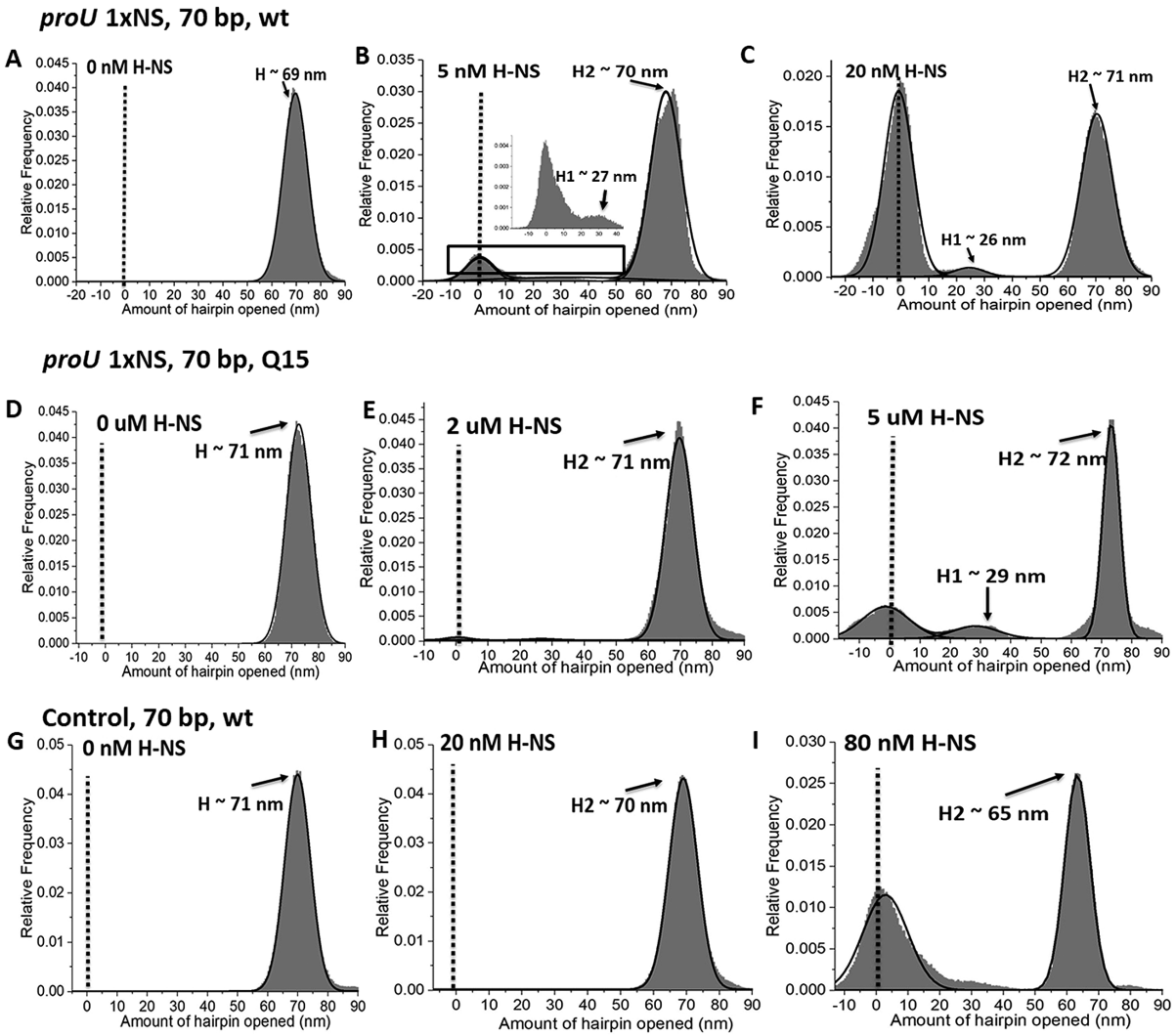

Figure 5. *proU* nucleation site-dependent local H-NS spreading. The distribution of the amount of hairpin opened of the 70 bp *proU* nucleation site (*proU* 1xNS, 70 bp) in the presence of wt H-NS at 0 nM (**A**), 5 nM (**B**) and 20 nM (**C**). The dotted line indicates the position at which the hairpin was completely closed. A sudden change in the relative size of the peaks corresponded to bound H-NS, and indicated a high degree of cooperativity. Distribution plots in the presence of the Q15 mutant at 0 μM (**D**), 2 μM (**E**) and 5 μM (**F**) and the distribution of the amount of hairpin opened of the 70 bp control sequence in the presence of wt H-NS at 0 nM (G), 20 nM (H) and 80 nM (I).

understanding of the molecular mechanisms behind DNA binding and gene silencing functions of H-NS.

SUPPLEMENTARY DATA

Supplementary Data are available at NAR Online.

ACKNOWLEDGEMENTS

We thank the protein expression core facility of the Mechanobiology Institute for protein purification. J.Y. and L.J.K. conceived the research. J.Y. and R.G. designed the single-molecule assay. Y.G. and L.J.K. designed the protein constructs. R.G. performed the experiments. R.G., L.J.K. and J.Y. interpreted the data and wrote the paper.

FUNDING

National Research Foundation, Prime Minister's Office, Singapore and the Ministry of Education under the Research Centres of Excellence programme [to J.Y. and L.J.K.]; VA [IOBX-000372 to L.J.K.]; NIH [AI123640]. Funding for open access charge: National Research Foundation, Prime Minister's Office, Singapore and the Ministry of Education under the Research Centres of Excellence programme [to J.Y.].
Conflict of interest statement. None declared.

REFERENCES

1. McCutcheon,J.P. and vonDohlen,C.D. (2011) An interdependent metabolic patchwork in the nested symbiosis of mealybugs. *Curr. Biol.*, **21**, 1366–1372.
2. Van Leuven,J.T., Meister,R.C., Simon,C. and McCutcheon,J.P. (2014) Sympatric speciation in a bacterial endosymbiont results in two genomes with the functionality of one. *Cell*, **158**, 1270–1280.

3. Han,K., Li,Z.-F., Peng,R., Zhu,L.-P., Zhou,T., Wang,L.-G., Li,S.-G., Zhang,X.-B., Hu,W., Wu,Z.-H. *et al.* (2013) Extraordinary expansion of a Sorangium cellulosum genome from an alkaline milieu. *Scientific Rep.*, **3**, 2101.
4. Azam,T.A. and Ishihama,A. (1999) Twelve species of the nucleoid-associated protein from Escherichia coli sequence recognition specificity and DNA binding affinity. *J. Biol. Chem.*, **274**, 33105–33113.
5. Luijsterburg,M.S., Noom,M.C., Wuite,G.J. and Dame,R.T. (2006) The architectural role of nucleoid-associated proteins in the organization of bacterial chromatin: a molecular perspective. *J. Struct. Biol.*, **156**, 262–272.
6. Dorman,C.J. (2009) Nucleoid-associated proteins and bacterial physiology. *Adv. Appl. Microbiol.*, **67**, 47–64.
7. Browning,D.F., Grainger,D.C. and Busby,S.J. (2010) Effects of nucleoid-associated proteins on bacterial chromosome structure and gene expression. *Curr. Opin. Microbiol.*, **13**, 773–780.
8. Dillon,S.C. and Dorman,C.J. (2010) Bacterial nucleoid-associated proteins, nucleoid structure and gene expression. *Nat.Rev.Microbiol.*, **8**, 185-195 .
9. Stoebel,D.M., Free,A. and Dorman,C.J. (2008) Anti-silencing: overcoming H-NS-mediated repression of transcription in Gram-negative enteric bacteria. *Microbiology*, **154**, 2533–2545.
10. Atlung,T. and Ingmer,H. (1997) H-NS: a modulator of environmentally regulated gene expression. *Mol. Microbiol.*, **24**, 7–17.
11. Dorman,C.J. (2007) H-NS, the genome sentinel. *Nat. Rev.Microbiol.*, **5**, 157-161.
12. Dorman,C.J., Hinton,J.C. and Free,A. (1999) Domain organization and oligomerization among H-NS-like nucleoid-associated proteins in bacteria. *Trends Microbiol.*, **7**, 124–128.
13. Schröder,O. and Wagner,R. (2002) The bacterial regulatory protein H-NS-a versatile modulator of nucleic acid structures. *Biol. Chem.*, **383**, 945–960.
14. Tendeng,C. and Bertin,P.N. (2003) H-NS in Gram-negative bacteria: a family of multifaceted proteins. *Trends Microbiol.*, **11**, 511–518.
15. Esposito,D., Petrovic,A., Harris,R., Ono,S., Eccleston,J.F., Mbabaali,A., Haq,I., Higgins,C.F., Hinton,J.C., Driscoll,P.C. *et al.* (2002) H-NS oligomerization domain structure reveals the mechanism for high order self-association of the intact protein. *J. Mol. Biol.*, **324**, 841–850.
16. Arold,S.T., Leonard,P.G., Parkinson,G.N. and Ladbury,J.E. (2010) H-NS forms a superhelical protein scaffold for DNA condensation. *Proc. Natl. Acad. Sci. U.S.A.*, **107**, 15728–15732.
17. Amit,R., Oppenheim,A.B. and Stavans,J. (2004) Single molecule elasticity measurements: a biophysical approach to bacterial nucleoid organization. *Biophys.J.*, **87**, 1392-1393.
18. Amit,R., Oppenheim,A.B. and Stavans,J. (2003) Increased bending rigidity of single DNA molecules by H-NS, a temperature and osmolarity sensor. *Biophys. J.*, **84**, 2467–2473.
19. Liu,Y., Chen,H., Kenney,L.J. and Yan,J. (2010) A divalent switch drives H-NS/DNA-binding conformations between stiffening and bridging modes. *Genes Dev.*, **24**, 339–344.
20. Winardhi,R.S., Gulvady,R., Mellies,J.L. and Yan,J. (2014) Locus of enterocyte effacement-encoded regulator (Ler) of pathogenic Escherichia coli competes off nucleoid structuring protein H-NS through non-cooperative DNA binding. *J.Biol.Chem.*, 13739–13750.
21. Walthers,D., Li,Y., Liu,Y., Anand,G., Yan,J. and Kenney,L.J. (2011) Salmonella enterica response regulator SsrB relieves H-NS silencing by displacing H-NS bound in polymerization mode and directly activates transcription. *J. Biol. Chem.*, **286**, 1895–1902.
22. Lim,C.J., Lee,S.Y., Kenney,L.J. and Yan,J. (2012) Nucleoprotein filament formation is the structural basis for bacterial protein H-NS gene silencing. *Scientific Rep.*, **2**, 509.
23. Winardhi,R.S., Fu,W., Castang,S., Li,Y., Dove,S.L. and Yan,J. (2012) Higher order oligomerization is required for H-NS family member MvaT to form gene-silencing nucleoprotein filament. *Nucleic Acids Res.*, **40**, 8942–8952.
24. Qu,Y., Lim,C.J., Whang,Y.R., Liu,J. and Yan,J. (2013) Mechanism of DNA organization by Mycobacterium tuberculosis protein Lsr2. *Nucleic Acids Res.*, **41**, 5263–5272.
25. Winardhi,R.S., Yan,J. and Kenney,L.J. (2015) H-NS regulates gene expression and compacts the nucleoid: insights from single-molecule experiments. *Biophys. J.*, **109**, 1321–1329.
26. Ali,S.S., Xia,B., Liu,J. and Navarre,W.W. (2012) Silencing of foreign DNA in bacteria. *Curr. Opin. Microbiol.*, **15**, 175–181.
27. Oshima,T., Ishikawa,S., Kurokawa,K., Aiba,H. and Ogasawara,N. (2006) Escherichia coli histone-like protein H-NS preferentially binds to horizontally acquired DNA in association with RNA polymerase. *DNA Res.*, **13**, 141–153.
28. Lucchini,S., Rowley,G., Goldberg,M.D., Hurd,D., Harrison,M. and Hinton,J.C. (2006) H-NS mediates the silencing of laterally acquired genes in bacteria. *PLoS Pathogens*, **2**, e81.
29. Navarre,W.W., Porwollik,S., Wang,Y., McClelland,M., Rosen,H., Libby,S.J. and Fang,F.C. (2006) Selective silencing of foreign DNA with low GC content by the H-NS protein in Salmonella. *Science*, **313**, 236–238.
30. Ding,P., McFarland,K.A., Jin,S., Tong,G., Duan,B., Yang,A., Hughes,T.R., Liu,J., Dove,S.L., Navarre,W.W. *et al.* (2015) A novel AT-rich DNA recognition mechanism for bacterial xenogeneic silencer MvaT. *PLoS Pathogens*, **11**, e1004967.
31. Lang,B., Blot,N., Bouffartigues,E., Buckle,M., Geertz,M., Gualerzi,C.O., Mavathur,R., Muskhelishvili,G., Pon,C.L., Rimsky,S. *et al.* (2007) High-affinity DNA binding sites for H-NS provide a molecular basis for selective silencing within proteobacterial genomes. *Nucleic Acids Res.*, **35**, 6330–6337.
32. Bouffartigues,E., Buckle,M., Badaut,C., Travers,A. and Rimsky,S. (2007) H-NS cooperative binding to high-affinity sites in a regulatory element results in transcriptional silencing. *Nat. Struct.Mol.Biol.*, **14**, 441-448.
33. Ueguchi,C., Seto,C., Suzuki,T. and Mizuno,T. (1997) Clarification of the dimerization domain and its functional significance for the Escherichia coli nucleoid protein H-NS.*J. Mol. Biol.*, **274**, 145–151.
34. Ueguchi,C., Suzuki,T., Yoshida,T., Tanaka,K.-i. and Mizuno,T. (1996) Systematic mutational analysis revealing the functional domain organization of Escherichia coli nucleoid protein H-NS. *J. Mol. Biol.*, **263**, 149–162.
35. Smyth,C.P., Lundbäck,T., Renzoni,D., Siligardi,G., Beavil,R., Layton,M., Sidebotham,J.M., Hinton,J.C., Driscoll,P.C., Higgins,C.F. *et al.* (2000) Oligomerization of the chromatin-structuring protein H-NS. *Mol. Microbiol.*, **36**, 962–972.
36. Gao,Y., Foo,Y.H., Winardhi,R.S., Tang,Q., Yan,J. and Kenney,L.J. (2017) Charged residues in the H-NS linker drive DNA binding and gene silencing in single cells. *Proc. Natl. Acad. Sci. U.S.A.*, **114**, 12560–12565.
37. Zhao,X., Peter,S., Dröge,P. and Yan,J. (2017) Oncofetal HMGA2 effectively curbs unconstrained (+) and (-) DNA supercoiling. *Scientific Rep.*, **7**, 8440.
38. Manosas,M., Camunas-Soler,J., Croquette,V. and Ritort,F. (2017) Single molecule high-throughput footprinting of small and large DNA ligands. *Nat. Commun.*, **8**, 304.
39. Woodside,M.T., Behnke-Parks,W.M., Larizadeh,K., Travers,K., Herschlag,D. and Block,S.M. (2006) Nanomechanical measurements of the sequence-dependent folding landscapes of single nucleic acid hairpins. *Proc. Natl. Acad. Sci. U.S.A.*, **103**, 6190–6195.
40. Desai,S.K., Winardhi,R.S., Periasamy,S., Dykas,M.M., Jie,Y. and Kenney,L.J. (2016) The horizontally-acquired response regulator SsrB drives a Salmonella lifestyle switch by relieving biofilm silencing. *Elife*, **5**, e10747.
41. Shindo,H., Ohnuki,A., Ginba,H., Katoh,E., Ueguchi,C., Mizuno,T. and Yamazaki,T. (1999) Identification of the DNA binding surface of H-NS protein from Escherichia coli by heteronuclear NMR spectroscopy. *FEBS Lett.*, **455**, 63–69.
42. Gordon,B.R., Li,Y., Cote,A., Weirauch,M.T., Ding,P., Hughes,T.R., Navarre,W.W., Xia,B. and Liu,J. (2011) Structural basis for recognition of AT-rich DNA by unrelated xenogeneic silencing proteins. *Proc. Natl. Acad. Sci. U.S.A.*, **108**, 10690–10695.